JOURNAL OF CATALYSIS 18, 90–107 (1970)

A Mössbauer Spectroscopic Study of the Reversible Oxidation of Ferrous Ions in Y Zeolite

R. L. GARTEN,* W. N. DELGASS,† AND M. BOUDART**

Laboratory for the Study of Adsorption and Catalysis, Stanford University, Stanford, California 94305

Received September 26, 1969

The ferrous ions in dehydrated Fe^{2+}–Y zeolite are oxidized to ferric ions by the adsorption of dry oxygen at 400°C. Approximately one oxygen atom is adsorbed for two iron ions. It is proposed that the oxidation at 400°C forms iron–oxygen–iron bridges inside the sodalite cages. The adsorption of water, ethanol, ammonia, and piperidine on the oxidized iron zeolite are discussed in terms of the proposed model. The adsorbed oxygen can be removed by hydrogen reduction at 400°C with restoration of the original material. Much of the adsorbed oxygen is removed by evacuation of the oxidized material at 525°C with partial regeneration of the same ferrous species observed in dehydrated Fe^{2+}–Y. Oxidation of Fe^{2+}–Y at room temperature in wet oxygen leads to partial formation of ferric ions. The results of this study are in good agreement with those obtained by others who started with a Fe^{3+}-exchanged Y zeolite.

INTRODUCTION

Mössbauer spectroscopy has now been employed in several investigations to study the chemical states and local environments of iron ions exchanged into zeolites (*1–5*). Several different zeolite structures have been investigated, but in particular, the near-faujasite or Y-type zeolites have received considerable attention because of their importance in adsorption and catalysis. The Y-type zeolite is a crystalline aluminosilicate whose internal void volume is made up of cages of known size as determined by X-ray diffraction studies. The Y form of zeolite is characterized by three different cages: the hexagonal prism, sodalite cage, and supercage (see Fig. 8). Each supercage opens tetrahedrally into four other supercages through an opening of about 9 Å forming a three-dimensional interconnecting network which produces a large internal surface area. In the hydrated state the zeolite cavities are filled with water which forms an intracrystalline fluid (*6*). More detailed and complete descriptions of the structure and properties of Y-type zeolite have been given in review articles (*7*, *8*).

Most of the Mössbauer studies of iron Y zeolites have been concerned with the effects of dehyration on the chemical states of the zeolite iron ions. Some studies of the adsorption of molecules at room temperature on dehydrated iron zeolites have been reported, however, and adsorption effects have been observed. Thus Gol'danskii and co-workers (*1*) observed the appearance of Fe^{2+} lines in the spectrum of Fe^{3+}–Y zeolite, whose state of hydration was not given, when $(CH_3)_4Sn$, C_2H_5OH, and C_6H_{14} were adsorbed at room temperature. These authors suggested that the adsorption

* Present address: Corporate Research Laboratories, Esso Research and Engineering Company, P. O. Box 45, Linden, N. J. 07036.

† Present address: Department of Engineering and Applied Science, Yale University, New Haven, Connecticut 06520.

** To whom queries concerning this paper should be sent: Department of Chemical Engineering, Stanford University, Stanford, California 94305.

process led to a localization of Fe^{2+} ions which were present in the zeolite in an unbound state before the adsorption. Morice and Rees (*3*) observed that dehydration of an Fe^{3+}-exchanged Y zeolite led to the formation of two types of ferrous ions but did not explain the reduction process in detail. Exposure of the sample to air or methanol caused reoxidation of the ferrous ions to ferric ions and gave a spectrum similar to that of the initially prepared Fe^{3+}–Y. Delgass *et al.* (*5*), in studies of dehydrated Fe^{2+}-exchanged Y zeolite, observed two chemical states of ferrous ion whose Mössbauer parameters were in good agreement with those observed by Morice and Rees (*3*). Delgass *et al.* (*5*) used the adsorption of molecules of varying size and reactivity to probe the zeolite structure and to obtain information on the accessibility and locations of the ferrous ions in the zeolite. In this case, advantage was taken of the "molecular sieve" properties and known crystal structure of the Y zeolite framework.

Although changes in Mössbauer spectra as a result of the adsorption of molecules from the gas phase have been observed, little information on the nature of the "adsorption complex" between the Mössbauer atom and the adsorbate molecule has been obtained. This results from the fact that in the investigations cited above it was not possible to resolve the "product peaks" from the spectra taken after adsorption. The present paper reports our observation, by Mössbauer spectroscopy, of the "product peaks" resulting from the adsorption of oxygen on iron ions in dehydrated Fe^{2+}–Y zeolite at 400°C. In addition, Mössbauer data, volumetric adsorption data, and previous Mössbauer studies of dehydrated Fe^{2+}–Y zeolite have led to a model for the "adsorption complex."

Experimental Methods

The iron zeolites were prepared by treating the sodium form of Linde Y zeolite with an aqueous solution of $FeSO_4$ in a nitrogen atmosphere (*4*). The composition of the Na–Y starting material was (%): Na_2O, 12.99; Al_2O_3, 22.19; and SiO_2, 64.82 on a dry weight basis. Examination with X-rays showed the iron zeolite samples to be crystalline before and after all experiments. The crystallinity of the freshly prepared Fe^{2+}–Y samples was also checked by determining nitrogen uptakes at liquid nitrogen temperature and at a relative pressure (P/P_0) of ~0.1 on dehydrated samples. The nitrogen uptakes and chemical analyses of the samples used in this investigation are reported in Table 1. Agreement between the nitrogen uptakes for the exchanged samples and the Na–Y starting material indicates that the high internal surface area and, therefore, the crystallinity of the zeolite was maintained after the iron exchange.

TABLE 1
Analysis of Samples and Nitrogen Saturation Volumes

The value given in parentheses indicates % exchange.

Sample	% Na	% Fe	% Al	N_2(mmole/g) uptake at 78°K and $P/P_0 \sim 0.1$
Na–Y	9.6	—	11.74	9.45
Fe–Y(71)	2.03	8.35	—	9.28
Fe–Y(65)	2.83	7.72	11.40	9.05
Fe–Y(58)	3.45	6.80	11.38	9.39
Fe–Y(31)	—	3.66	—	9.01

The Mössbauer absorbers were made by pressing, at 10000 psi, 0.2–0.3 g of wet iron zeolite into a ½ or ⅝-in. wafer. The absorber wafer was placed in a Mössbauer cell which was designed for both temperature and atmosphere control. The temperature was measured by a thermocouple located near the absorber. The design of the cell has been described in more detail elsewhere (*9*).

The zeolite wafers were dehydrated according to the following procedure. The samples were first evacuated at room temperature for 4–12 hr to a vacuum of 10^{-4}–10^{-5} Torr. The temperature was then raised to 400°C over a period of 6–8 hr with at least 1 hr spent at 100°C; and the sample was evacuated at 400°C for 4–12 hr to a final pressure of 10^{-5}–10^{-6} Torr.

In some experiments, the iron zeolite was dehydrated in flowing helium, which had been dried by passage through a Dry Ice–acetone trap, according to the heating schedule described above. A second Mössbauer cell, made from a Pyrex tube with thinned glass windows and stainless steel valves on the inlet and outlet, was employed in the helium flow experiments. The absorber wafer was mounted in an aluminum holder which was held in place by copper leaf springs. The samples were heated *in situ* by a removable external furnace, and the temperature was measured by a thermocouple located near the absorber wafer but outside the cell.

The Mössbauer spectra were taken on an automechanical constant velocity spectrometer using a ^{57}Co–Cr source. All isomer shifts are reported with respect to the ^{57}Co–Cr source. Positive velocity corresponds to the source moving toward the absorber. The data from each run were submitted to least squares analysis by a version of the Argonne variable metric minimization Mössbauer data fitting program. The background radiation was estimated at the beginning of each run by counting at a nonresonant velocity with a 4.5-mil brass foil between the source and absorber. Spectral areas were calculated from the least squares fit parameters and were corrected for the signal-to-noise ratio measured by the brass foil technique (*4*).

The oxygen adsorption measurements were made on a conventional adsorption apparatus which has been described previously (*10*). One- to 2-g samples of zeolite were placed in an adsorption bulb which had a thermocouple well extending into the adsorbent bed. The zeolite samples were attached to the adsorption apparatus and evacuated as the temperature was raised to 400°C over a period of 24 hr. The samples were finally evacuated for 12 hr at 400–415°C. Oxygen uptakes were then determined at 400°C on the freshly dehydrated samples. Following the oxygen adsorption the oxidized samples were cooled to room temperature and then treated in flowing hydrogen as the temperature was raised to 400°C over a period of ~2 hr. Hydrogen treatment was continued for at least 1 hr followed by outgassing of the sample at 400°C to $\sim 10^{-5}$ Torr. The oxygen uptakes were then repeated on the reduced samples. The oxygen used was of 99.5% purity and was distilled from a liquid nitrogen trap and hydrogen was diffused through a palladium thimble followed by a liquid nitrogen trap.

In the Mössbauer experiments oxygen of 99.5% purity was passed through a Dry Ice–acetone trap while hydrogen was passed through a Deoxo unit followed by a Dry Ice–acetone trap. Ammonia of 99.5% purity was obtained from the Matheson Company. The ammonia was condensed in a trap held at liquid nitrogen temperature, degassed by freeze–thaw–freeze–evacuation cycles and retained in a storage bulb. The ethanol and piperidine were reagent grade materials. Small amounts of these liquids were degassed by freeze–thaw–freeze–evacuation cycles. Ethanol was then dried by passage through a silica gel trap at room temperature and immediately admitted to the zeolite absorber. Piperidine was passed through sodium hydroxide pellets followed by silica gel before being admitted to the zeolite absorber.

Results

Characteristics Spectrum of Dehydrated Fe^{2+}–Y Zeolite

Figure 1a shows the characteristic room temperature spectrum of Fe^{2+}–Y zeolite obtained after heating the material under vacuum or in dried flowing helium at 400°C for 2 hr or more. A detailed discussion of this spectrum is given in Ref. (*5*). The *outer* peaks constitute a broad doublet with isomer shift (IS), 1.40 mm/sec (^{57}Co–Cr), and quadrupole splitting (QS), 2.36 mm/sec. The *inner* peaks are attributed to a doublet with IS, 1.04 mm/sec (^{57}Co–Cr) and QS, 0.62 mm/sec. The room temperature adsorption of molecules such as piperidine, *t*-butyl alcohol, ethanol, and CS_2 which are small enough to enter the supercages but too large to enter the sodalite cages or hexagonal prisms of the zeolite removed the *inner* peaks from the Möss-

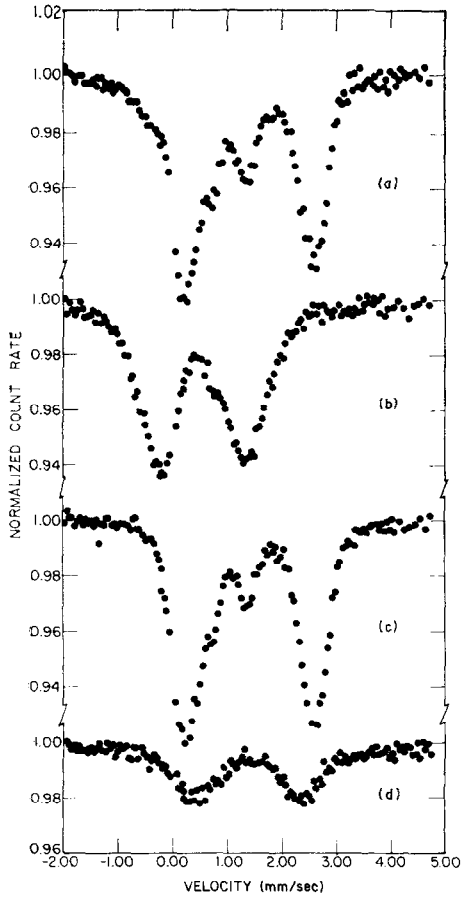

FIG. 1. Oxidation–reduction of iron Y zeolite: (a) Fe^{2+}–Y dehydrated at 400°C; (b) oxidized at 400°C; (c) reduced in hydrogen at 400°C; (d) exposed to 15 Torr H_2O. All spectra at room temperature and on the same sample.

bauer spectrum. In these cases only slight perturbations on the *outer* peaks were observed. The *inner* and *outer* peaks were strongly affected, however, by the adsorption of small molecules such as NH_3 and H_2O which are small enough to enter all the cages of the zeolite.

Oxidation of Fe^{2+}–Y Zeolite in Dry Oxygen at 400°C

When the sample giving the characteristic spectrum of Fig. 1a was exposed at room temperature to 760 Torr of dry oxygen, nitrogen, or hydrogen for ~12 hr, no changes were observed in the Mössbauer spectrum. Treatment of the same sample in dried flowing oxygen for 0.5 hr at 400°C, however, changed the chemical state of the iron in the zeolite as shown in Fig. 1b. From a chemical point of view one would expect that the high temperature treatment in oxygen would convert the zeolite ferrous ions to ferric ions. The IS of the two lines taken as a doublet falls in the range expected for ferric ions. We therefore assign the two broad lines of Fig. 1b to a ferric quadrupole doublet. The widths of the broad lines were not a function of temperature, indicating that a distribution of iron environments was present.

Room temperature spectra for 11 different oxidized samples were analyzed by computer fitting. Poor reproducibility of the resolved line positions and, in many cases, parameters without physical meaning were found for a four- or six-line fit to the Mössbauer data. Fitting with two lines, however, gave fair reproducibility of the line positions, but in general, poor chi-square values (a measure of the goodness of fit) were obtained. Based on the 11 different samples of oxidized iron zeolite an IS of 0.57 ± 0.03 mm/sec (^{57}Co–Cr) and a QS of 1.66 ± 0.06 mm/sec was determined. The errors are the average deviations of the 11 runs used.

The temperature dependence of the Mössbauer spectrum of oxidized iron Y zeolite is shown in Fig. 2a–c for the temperature range 25°C to 400°C. The QS of the doublet decreased slightly with temperature giving the values 1.63, 1.57, and 1.50 mm/sec at 25, 223, and 400°C, respectively. The temperature dependence of the IS was $\sim -6.4 \times 10^{-4}$ mm/sec°C. This value is within the range expected for the second-order Doppler shift of ferric ions in various oxides (*11*). The IS of the doublet was 0.58, 0.44, and 0.34 mm/sec (^{57}Co–Cr) at 25, 223, and 400°C, respectively.

From the spectra of Fig. 2, a Debye temperature of ~280°K for the oxidized iron zeolite was estimated by plotting the logarithm of the total area under the Mössbauer absorption curve *versus* temperature. Since this value is only an estimate it is not considered to the significantly different from the value of 250°K found for dehydrated Fe^{2+}–Y zeolite (*5*).

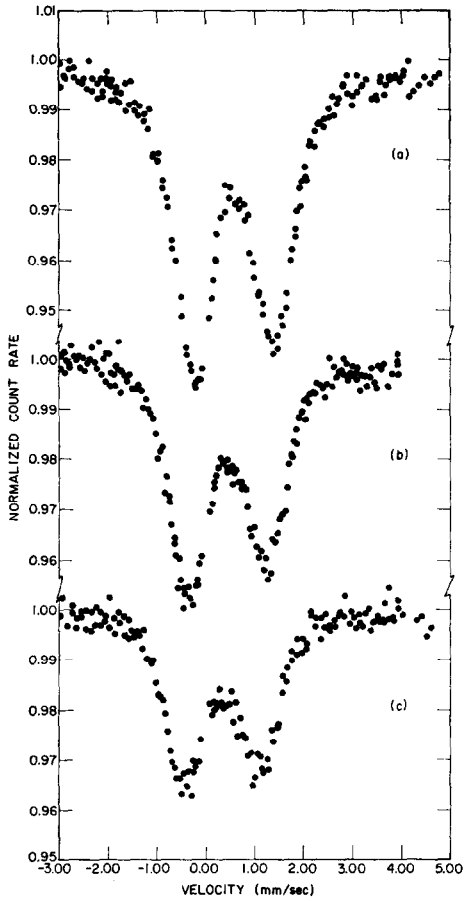

FIG. 2. Temperature dependence of the Mössbauer spectrum of oxidized iron Y zeolite (°C): (a) 25; (b)223; (c) 400. All spectra on the same sample.

Reduction of the Oxidized Iron Zeolite

The sample of Fig. 1b was treated in flowing hydrogen as the sample temperature was slowly raised from room temperature to 440°C. The hydrogen treatment was then continued for 5 hr at this temperature. Figure 1c shows that this treatment reduced the zeolite iron ions to the ferrous state and produced once again the characteristic spectrum of the original dehydrated material. Exposing the reduced sample of Fig. 1c to 15 Torr of water vapor to saturate the zeolite cavities led to a large decrease in spectral area as shown in 1d. Based on previous work (*4*), this result is taken as an indication that the ion exchange character of the iron ions has been maintained after the oxidation and reduction. It should be noted that the hydrogen treatment at 440°C did not reduce the zeolite iron below the ferrous state.

Part of the ferric ions in the oxidized iron zeolite was reduced to the ferrous state by evacuation of the sample at elevated temperature. This is illustrated in Fig. 3a–c. The oxygen which was adsorbed in oxidizing the zeolite iron ions was fairly stable to evacuation for 3.25 hr at 400°C (Fig. 3b). The spectrum of Fig. 3b, however, is not identical to that of 3a since new peaks are evident. Computer resolution of spectrum 3b for six lines did not give meaningful results but a four-line fit showed new peaks at 0.1 and 0.8 mm/sec in addition to the peaks of the ferric doublet.

Evacuation of the same sample at 525°C for 9 hr desorbed much of the oxygen as shown in spectrum 3c. Comparison of Fig. 3c with 3a and 1a shows that some of the iron was still present in the oxidized state but that much of the iron had been reduced to the ferrous state. Computer fitting for

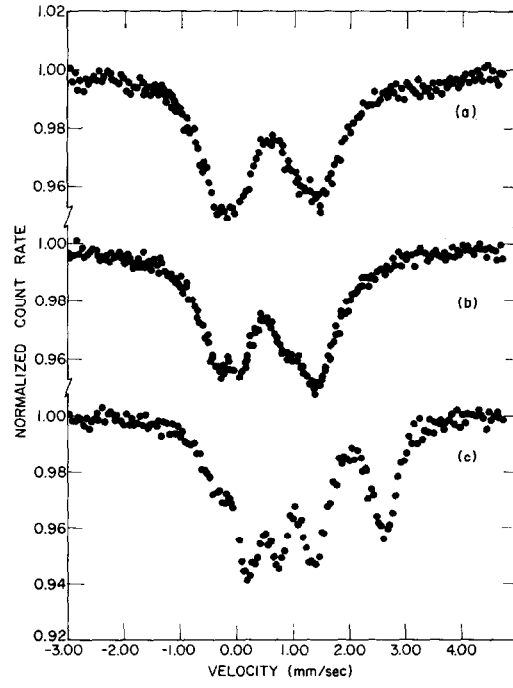

FIG. 3. Effect of evacuation on oxidized iron zeolite: (a) oxidized at 430°C, 7 hr; (b) evacuated at 400°C, 3.25 hr; (c) evacuated at 525°C, 9 hr. All spectra at room temperature on the same sample.

six lines resolved three doublets in spectrum 3c. Doublet 1 with IS, 0.54 mm/sec (^{57}Co–Cr), and QS, 1.84 mm/sec, is assigned to Fe^{3+} ion. The QS is somewhat larger than that found for Fe^{2+}–Y oxidized at 400°C in dry oxygen (Fig. 1b), but this may be due to the presence of ferrous ions or to difficulties of resolving the lines of the more complex spectrum in Fig. 3c. Doublet 2 with IS, 1.00 mm/sec (^{57}Co–Cr), and QS, 0.51 mm/sec; and Doublet 3 with IS, 1.41 mm/sec (^{57}Co–Cr), and QS, 2.40 mm/sec, are identified as the *inner* and *outer* peaks of the characteristic spectrum of dehydrated Fe^{2+}–Y.

Oxygen Uptake on Dehydrated Fe^{2+}–Y

Volumetric adsorption measurements of oxygen on dehydrated Fe^{2+}–Y were made to determine oxygen atom to iron ion ratios. Oxygen uptakes were determined at 400°C on 1.220 g of a high exchanged sample, Fe^{2+}–Y(65), containing 1328 μmole of Fe/g of dry zeolite and on 1.805 g of a low exchanged sample, Fe^{2+}–Y(31), containing 655.4 μmole of Fe/g of dry zeolite. The oxygen uptakes were determined on freshly dehydrated samples and repeated after hydrogen reduction of the oxidized samples. The uptake of oxygen by the Fe^{2+}–Y samples required several hours for completion. However, approximately 90% of the total oxygen adsorbed was taken up in the first 30 min of exposure.

Figure 4 shows the oxygen uptakes as a function of pressure on freshly dehydrated Fe^{2+}–Y(31) and Fe^{2+}–Y(65) samples and after reduction of the oxidized samples. The uptakes were practically independent of pressure over the range studied. Extrapolation to zero oxygen pressure gave O/Fe atom ratios of 0.43 for Fe^{2+}–Y(65) and 0.49 for Fe^{2+}–Y(31).

Nitrogen saturation volumes at liquid nitrogen temperature on the oxidized sample of Fe^{2+}–Y(65) gave a value of 9.04 mmole of N_2/g at $P/P_0 \sim 0.1$ and a value of 8.96 mmole of N_2/g at $P/P_0 \sim 0.1$ for the oxidized and reduced sample of Fe^{2+}–Y(31). These results show that the high internal surface area and, therefore, the crystallinity of the samples was maintained throughout the oxidation and reduction of the iron zeolite. No oxygen adsorption was detected on a dehydrated sample of Na–Y zeolite at 400°C.

Adsorption Interactions on Oxidized Iron Zeolite

When a 400°C oxidized iron zeolite was equilibrated with water at 15 Torr and room temperature to saturate the zeolite cavities, the QS of the Fe^{3+} doublet decreased from 1.66 to 0.84 mm/sec. This is shown in Fig. 5a,b. The IS of the doublet for the hydrated material is 0.52 mm/sec (^{57}Co–Cr) and is not significantly different from that of the oxidized iron zeolite of

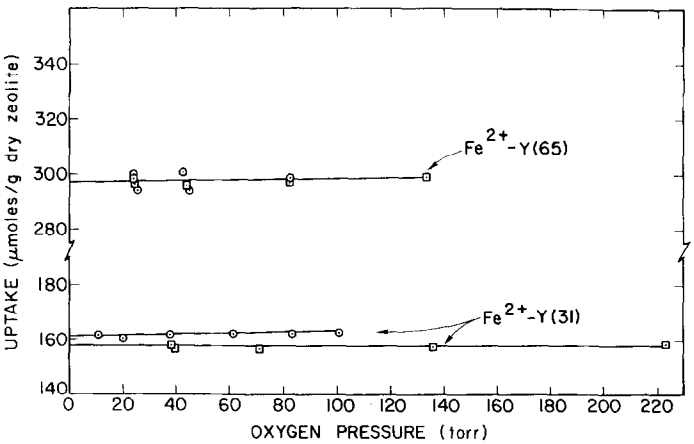

FIG. 4. Oxygen uptakes on Fe^{2+}–Y zeolite at 400°C: ⊙, dehydrated sample; ⊡, oxidized and reduced sample.

Fig. 5a. Hydration of the oxidized iron zeolite caused a decrease in spectral area of ~10%.

The effect of evacuating the hydrated oxidized iron zeolite at successively higher temperatures is shown in Fig. 5b–e. The QS of the Fe^{3+} doublet increases with increasing degree of dehydration. The QS is 0.82, 0.98, and 1.38 mm/sec for the wet, room temperature evacuated and 108°C evacuated samples, respectively. The sample evacuated for 2 hr at 500°C showed a continued increase in QS but new peaks appeared. The peaks at 0.8 and 2.6 mm/sec, which are close to the expected values for the left *inner* and right *outer* peaks of the characteristic spectrum, and the asymmetry in the broad absorption lines at ~—0.3 and ~1.3 mm/sec indicate that some reduction to ferrous ion has occurred. The reduction is due to the desorption of oxygen during evacuation at high temperature as was shown earlier (Fig. 3c). The shorter evacuation period and lower temperature used prior to spectrum of Fig. 5e could account for the smaller degree of reduction to the ferrous state. Reduction of the sample giving spectrum 5e in flowing hydrogen for 3 hr at 400°C followed by a 1 hr evacuation at 500°C, produced once again the characteristic spectrum of dehydrated Fe^{2+}–Y zeolite. This is taken as evidence that no irreversible reaction of the zeolite iron ions occurred during the oxidation–hydration–evacuation–reduction cycle.

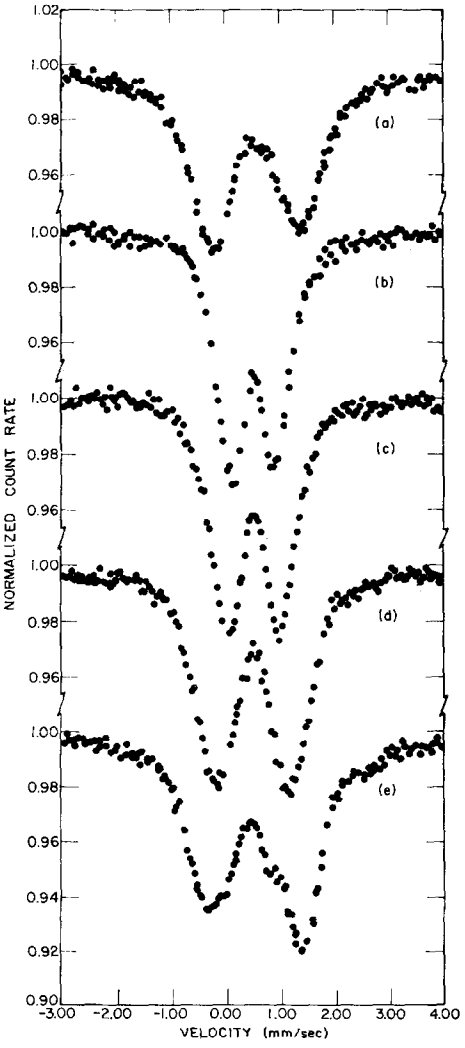

FIG. 5. Adsorption of water on oxidized iron zeolite followed by evacuation at various temperatures; (a) O_2, 400°C, 10 hr; (b) Torr H_2O, 25°C; (c) evacuated 25°C, 8 hr; (d) evacuated 108°C, 2 hr; (e) evacuated 500°C, 2 hr. All spectra at room temperature and on the same sample.

The effects of the adsorption of ammonia, ethanol, and piperidine on the oxidized iron zeolite are shown in Fig. 6a–c. In all cases the QS of the doublet decreased as a result of adsorption but the decrease was not as great as when water was adsorbed. Computer fitting of spectra 6a,b for two lines and 6c for three lines gave quadrupole splittings for the main doublet of 1.4, 1.3, and 1.2 mm/sec for ammonia, ethanol, and piperidine, respectively. The spectral area changes were a 15% decrease for NH_3 adsorption and increases of 9% and 6% for ethanol and piperidine adsorption, respectively. Spectrum 6c for piperidine adsorption clearly shows an additional peak at 2.3 mm/sec. Since we expect this peak to be the right half of a quadrupole doublet, a four-line computer fit was made in an attempt to resolve the two doublets. Such a fit resolved the left peak into two peaks of nearly equal intensity without significantly affecting the intensities of the two right peaks. This solution gives rise to two very asymmetrical quadrupole doublets. A four-line fit with the constraint that a peak equal in intensity to that of the right outer peak be located in the region —1.0 to +1.0 mm/

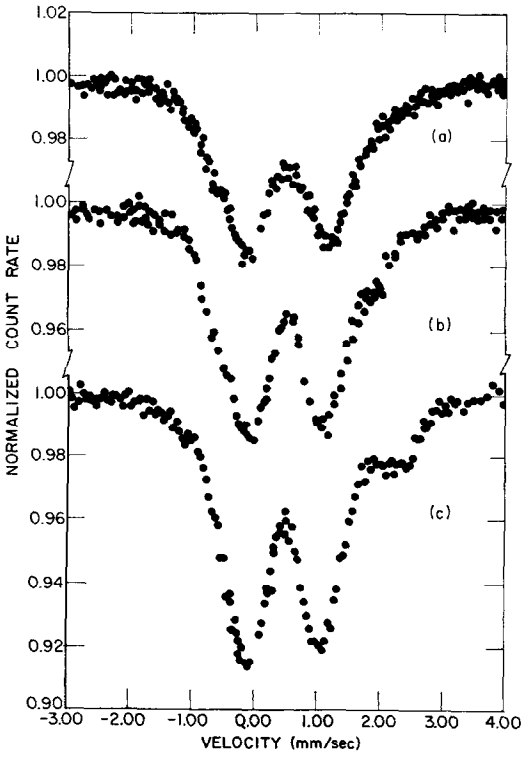

FIG. 6. Adsorption effects on oxidized iron zeolite: (a) 760 Torr ammonia; (b) 32 Torr ethanol; (c) 25 Torr piperidine. All spectra at room temperature on separate samples.

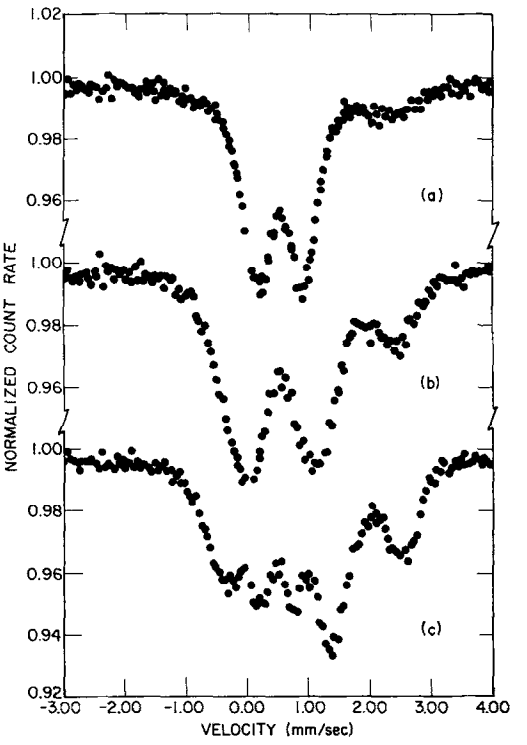

FIG. 7. Oxidation of Y zeolite at room temperature by air and water followed by evacuation at various temperatures. (a) exposed at 25°C to H_2O, 0.75 hr, air 12 hr; (b) evacuated 100°C, 10 hr; (c) evacuated 410°C, 2.5 hr. All spectra at room temperature and on the same sample.

sec did not improve the computer fit. We cannot, on the basis of the computer analysis, make assignments for the positions of four lines in spectrum 6c with any confidence and thus cannot determine the Mössbauer parameters of the iron species giving rise to the 2.3 mm/sec peak. The piperidine adsorption study does, however, indicate the presence of at least two types of iron in the oxidized iron zeolite.

No additional lines are visible in the spectra for ammonia and ethanol adsorption, and differential spectra (*5*), determined by substracting the spectrum before adsorption from that taken after adsorption, did not indicate the presence of additional lines.

Oxidation of Fe^{2+}–Y Zeolite at Room Temperature

Treatment of a dehydrated Fe^{2+}–Y sample in water vapor at room temperature by passing nitrogen at 100 ml/min through a water bubbler and over the sample for 0.75 hr followed by exposure to the air for 12 hr, oxidized most of the iron in the zeolite to the ferric state. This is shown in Fig. 7a. The 0.75 hr treatment in water vapor was sufficient to saturate the zeolite cavities. The exposure to water vapor and air did not oxidize all the zeolite iron since the small peak at 2.35 mm/sec indicates that some ferrous ions are still present. The area under the Mössbauer absorption curve of Fig. 7a is 33% less than that of the characteristic spectrum of the dehydrated Fe^{2+}–Y sample from which it was derived. This suggests, in light of previous work by us (*4*), that some of the ions were solvated in the zeolite water in 7a. It is probable that these were ferrous ions since we have shown (Fig. 5a–b) that the ferric ions in the high temperature

oxidized zeolite maintain strong bonds to the zeolite on hydration.

Figure 7b shows that evacuation of the sample from 7a at 100°C for 10 hr increased the QS of the ferric doublet and increased the intensity of the right outer peak due to ferrous ions. In addition the spectral area increased and became essentially the same as that of 7a. This agrees with the conclusion that some of the ferrous ions were solvated in the wet zeolite but were forced into localized positions by removing most of the water from the zeolite.

Evacuation of 7b for 2.5 hr at 410°C gave spectrum 7c. Spectrum 7c is interpreted in the same way as that of Fig. 3c and shows that much of the iron has been reduced to the ferrous state. The Mössbauer parameters of the three doublets, which were identified earlier in connection with Fig. 3c, are: Doublet 1, IS, 0.53 mm/sec (^{57}Co–Cr); QS, 1.85 mm/sec; Doublet 2, IS, 1.02 mm/sec (^{57}Co–Cr), QS, 0.55 mm/sec; Doublet 3, IS, 1.37 mm/sec (^{57}Co–Cr); QS, 2.32 mm/sec. Considering the time and temperature of evacuation, we see that the reduction to ferrous ion was easier in this case than for the samples of Figs. 3c and 5e.

Reduction of the sample of 7c at 400°C in hydrogen followed by evacuation for 9 hr at 400°C produced once again the characteristic spectrum of dehydrated Fe^{2+}–Y indicating that no irreversible changes occurred throughout the treatments of Fig. 7.

Oxidation of most of the ferrous ions to ferric ions also occurred when a room temperature evacuated sample of Fe^{2+}–Y was exposed to dry air for 11 hr. Room temperature evacuation removes ~½ of the zeolite water and forces the iron ions into localized positions. The water molecules, about four per iron ion in the half-hydrated sample, were sufficient to permit oxidation in the presence of oxygen.

Discussion

In a previous publication we presented a model to explain the characteristic Mössbauer spectrum of dehydrated Fe^{2+}–Y zeolite (*5*). In the present discussion we shall briefly summarize the essential features of that model and then consider the oxidized form of Fe^{2+}–Y zeolite in terms of the model. Next, adsorption interactions with the oxidized iron zeolite will be discussed and, finally, we shall compare the results of the present study with those obtained by others who started with Fe^{3+}-exchanged zeolite.

In dehydrated Fe^{2+}–Y zeolite, two different chemical states of iron were observed by Mössbauer spectroscopy. On the basis of the adsorption interactions with molecules of varying size, Mössbauer parameters and a comparison to Mössbauer data on other oxides, the *outer* peaks were assigned to ferrous ions in the hexagonal prism sites of the zeolite. In the same way, the *inner* peaks were assigned to ferrous ions in fourfold coordination near the hexagonal windows opening into the supercages. The fourfold coordinated iron is formed on dehydration of the zeolite at high temperature and is attributed to $Fe^{2+}(OH)^-$ and (or) Fe^{2+}–O^{2-}–Fe^{2+} groups in which each iron ion is also bonded to three framework oxygens. Two possible configurations for the fourfold

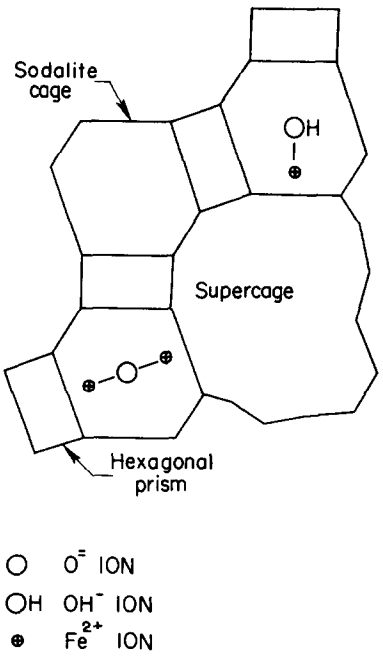

Fig. 8. Schematic diagram of fourfold coordinated ferrous ions in dehydrated Fe^{2+}–Y zeolite.

coordinated iron are shown in Fig. 8 while others are considered in Ref. (*5*).

With this model of dehydrated Fe^{2+}–Y zeolite in mind we now consider the oxidized form of the iron zeolite. The oxygen adsorption results which showed that approximately one oxygen atom was adsorbed for two zeolite iron ions and the Mössbauer spectra of the oxidized material leave little doubt that the 400°C oxygen treatment oxidized zeolite ferrous ions to ferric ions. The IS of the oxidized doublet is 0.58 mm/sec (^{57}Co–Cr), which falls within the range expected for high spin ferric ion. We know of no case where low spin Fe(III) has been observed in an oxide and, furthermore, the isomer shifts for low spin Fe(III) in a variety of compounds all fall below ~0.3 mm/sec (^{57}Co–Cr) (*12–14*). Since high spin Fe^{3+} is an *S*-state ion, $^6S_{5/2}$, the electric field gradient at the iron nucleus arises only from a surrounding noncubic charge distribution due to other ions in the crystal. Provided there are no phase changes or changes in the relative positions of the ions with temperature, the QS for high spin Fe^{3+} should be independent of temperature. The QS of the doublet from the 400°C oxidized material was nearly independent of temperature between 25 and 400°C. The slight decrease in QS that was observed may be due to small changes in the relative positions of the ions in the crystal as a function of temperature. The Mössbauer data are most consistent with an assignment of the doublet from the oxidized material to high spin ferric ion.

Previous Mössbauer studies of Fe^{3+} ions in a variety of oxides indicated that the IS can provide information on the coordination number of the ions (*11*). We have made a literature survey of Mössbauer data for Fe^{3+} ions in a variety of oxides. For the more than 50 compounds surveyed, isomer shifts for Fe^{3+} in fourfold coordination with oxygen fell below ~0.45 mm/sec (^{57}Co–Cr) while isomer shifts for Fe^{3+} in sixfold coordination were greater than ~0.45 mm/sec (^{57}Co–Cr). We found only three compounds which crossed the dividing line and there was not ready explanation for these exceptions. If we assume that the oxidized iron zeolite is not an exceptional case, the IS of 0.58 mm/sec (^{57}Co–Cr) indicates at least sixfold coordination for the Fe^{3+} ions giving rise to the doublet from the oxidized zeolite.

The Mössbauer spectra of the oxidized iron zeolite showed that most of the iron was affected by the 400°C treatment in oxygen. The oxygen adsorption results gave oxygen atom to iron ion ratios of ~1:2. Taken together, these results indicate that an adsorbed oxygen atom is complexed with more than one iron ion and that the oxidation involves the formation of Fe^{3+}–O^{2-}–Fe^{3+} bridges. The Fe^{3+} ions in these bridges are not exposed to molecules in the supercages of the zeolite since low heats of adsorption of krypton (2.9 kcal/mole) were obtained on the oxidized iron zeolite (*15*), and krypton is too large to enter the sodalite cages.

Consideration of the oxygen adsorption data, the Kr adsorption result, the IS of the Fe^{3+} doublet, and our previously proposed model for dehydrated Fe^{2+}–Y zeolite leads to the following model for the oxidized iron zeolite. Since the spectrum of dehydrated Fe^{2+}–Y indicated that most of the ferrous ions were in the hexagonal prisms (the outer peaks constitute ~75% of the spectral area in most dehydrated samples) the Fe^{3+}–O^{2-}–Fe^{3+} bridge in the oxidized zeolite must involve, for the most part, these ions. It seems unreasonable from a geometric and electrostatic point of view that two iron ions could remain in the center of the hexagonal prisms (sites *S I*)* and still be bonded to an adsorbed oxygen located inside the sodalite cage. It is more likely that the transfer of an electron from each of the two ferrous ions to an adsorbing oxygen would result in the movement of the iron ions from the center of the hexagonal prisms toward the same sodalite cage. The ferric ions could thus be located in the hexagonal windows of their corresponding hexagonal prisms and be bridged by the adsorbed oxide ion. This model is shown in Fig. 9A. In this configuration the Fe^{3+} ion is co-

* The site designations used here are the same as those used in Ref. (*16*).

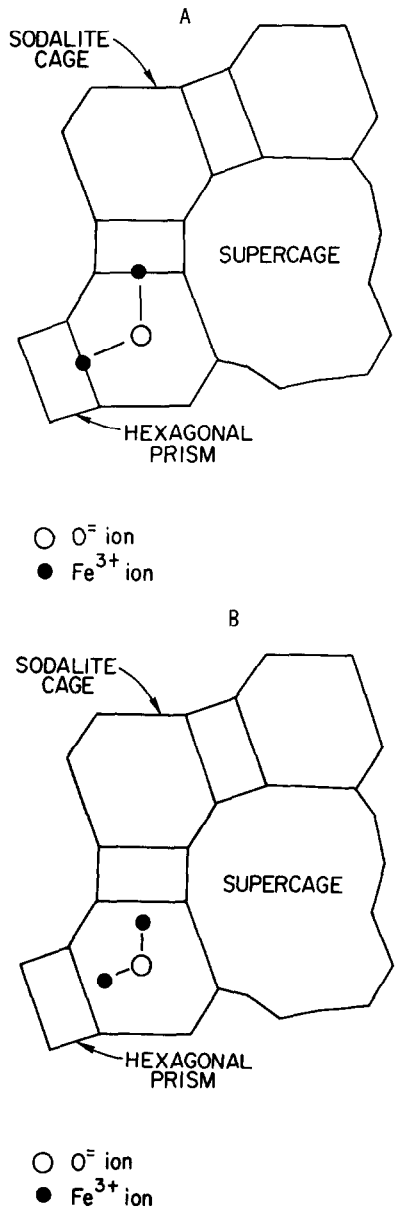

FIG. 9A. Schematic diagram of oxidized iron zeolite with Fe^{3+} ions in windows of hexagonal prisms. (B) Schematic diagram of oxidized iron zeolite with Fe^{3+} ions in *S I'* positions.

ordinated to seven oxygen ions and the measured IS is commensurate with such an assignment if the correlation between IS and coordination number applies. The charge distribution around the Fe^{3+} ion is asymmetrical and can account for the large QS of the oxidized species. Based on X-ray data for Na–Y zeolite (*17*), the configuration of Fig. 9A gives rise to a fairly long iron ion to adsorbed oxygen bond distance (~3.7 Å) if the adsorbed oxide ion is located in the center of the sodalite cage. This bond distance can be shortened somewhat by movement of the oxide ion along an axis which brings it closer to the Fe^{3+} ions but not so close to the framework oxygens that repulsion becomes important.

More favorable bond distances for the Fe^{3+} ions could be achieved by movement of the Fe^{3+} ions further toward the center of the sodalite cage into the *S I'* positions. This is illustrated in Fig. 9B. In this configuration the Fe^{3+} ions occupy sites of fourfold coordination. The Fe–O bond distances are ~2.7 and ~2.6 Å for the adsorbed oxygen and the O_3 oxygens [notation for oxygen positions is that used in Ref. (*17*)] of the hexagonal prism 6-ring, respectively. If this configuration is correct, then the IS of the oxidized zeolite represents an exception to the correlation between isomer shift and coordination number. A plausible explanation for a larger than expected IS for fourfold coordinated Fe^{3+} is found in the work of Šimánek and Šroubek (*18*). For iron in sixfold coordination with oxygen these authors showed that the electron density at the iron nucleus was a function of the Fe–O bond distance due to the overlap between the iron *s*-orbitals and the 2*p*-orbitals of the surrounding oxygens and also due to a change in the iron 4*s*-orbital occupation. An increase in the Fe–O bond distance was shown to decrease the electron density at the iron nucleus and, thus, increase the isomer shift. A similar effect was discussed for tetrahedral coordination. Normal bond distances for tetrahedral Fe^{3+} in various oxides are ~1.9 Å and, therefore, the configuration of Fig. 9B where the tetrahedron is expanded could give rise to a larger than expected IS. The results of Šimánek and Šroubek indicate that the correlation between coordination number and isomer shift should be used with caution especially in materials where abnormal bond distances may be enforced by a rigid lattice. Because of the more reasonable bond distances, previous evidence for the existence of the

SI' site for other trivalent cations (*16*, *19*) and the above explanation of the IS, we favor the configuration of Fig. 9B. The main feature of either model proposed above, however, is the formation of an Fe^{3+}–O^{2-}–Fe^{3+} bridge due to the adsorption of oxygen and the exact location of the ions will have to be determined by X-ray diffraction studies.

The next question which must be considered is whether the second kind of iron observed in the dehydrated Fe^{2+}–Y zeolite was oxidized. Comparison of the spectrum of a dehydrated Fe^{2+}–Y sample with the spectrum of the sample after oxidation shows that the right *inner* peak would overlap with the right half of the Fe^{3+} doublet but that the left *inner* peak should be resolved if it were still present with its original intensity. The left *inner* peak was not resolved in the spectra of the oxidized iron zeolite indicating that the chemical state of most of the iron giving rise to the *inner* peaks was altered by the oxidation. Further evidence which suggests that most of the *inner* peak species was oxidized is the area change on hydrating the oxidized iron zeolite. If the *inner* peak species were not oxidized, hydration of the oxidized iron zeolite should solvate these ions (*4*) and cause an area decrease. The area of the *inner* peaks in the dehydrated Fe^{2+}–Y sample was ~24% of the total area whereas the total area decrease on hydrating the oxidized iron zeolite was only ~10%. This result suggests that most of the *inner* peak species was oxidized. The 10% decrease in area on hydrating the oxidized sample could be due to some remaining ferrous ions or to a weakening effect of water on the Fe^{3+}–zeolite bonds. If the 10% area decrease was due to some of the *inner* peak iron species in the oxidized iron zeolite then only ~5% of the total area would be under each line of the *inner* peak doublet and these would be impossible to resolve from the broad doublet of the oxidized iron zeolite.

In the absence of additional information from the Mössbauer spectra of oxidized iron zeolite we can suggest possible paths for the oxidation of the *inner* peak iron species. In our model for dehydrated Fe^{2+}–Y zeolite the *inner* peaks were attributed to $Fe^{2+}(OH)^-$ groups near the hexagonal windows of the supercages and to Fe^{2+}–O^{2-}–Fe^{2+} bridges inside the sodalite cages. Oxidation of the $Fe^{2+}(OH)^-$ group could occur by formation of an Fe^{3+}–O^{2-}–$Fe^{3+}(OH)^-$ bridge involving an adjacent hexagonal prism ion. Since there are two hexagonal prism ions per sodalite cage, formation of an Fe^{2+}–O^{2-}–Fe^{2+} bridge between one of the prism ions and the hexagonal window $Fe^{2+}(OH)^-$ group as a result of dehydroxylation would leave the other prism Fe^{2+} ion isolated. Oxidation could then occur by breakage of the Fe^{2+}–O^{2-}–Fe^{2+} bridge with formation of an Fe^{3+}–O^{2-}–Fe^{3+} bridge, involving the prism ions, and an $Fe^{2+}O^{2-}$ group. This latter species would constitute only a small fraction of the total iron in the zeolite and would be difficult to resolve in the Mössbauer spectrum. Solvation of the $Fe^{2+}O^{2-}$ species could also account for the 10% area decrease observed on hydration of the oxidized iron zeolite.

From a catalytic standpoint, the important result of this work is the reversibility of the oxidation of the zeolite iron ions. The adsorbed oxygen was removed by reduction of the sample in hydrogen returning the iron ions to their original states and maintaining their ion exchange character without a loss of crystallinity. Much of the adsorbed oxygen was also removed by evacuation of the oxidized sample at high temperature returning the iron ions to the ferrous state and producing both the *inner* and *outer* peaks. Removal of the adsorbed oxygen by hydrogen or evacuation regenerates both the *inner* and *outer* peaks by reversing the steps suggested earlier for formation of the oxidized species. To our knowledge *this is the first observation, by Mössbauer spectroscopy, of a reversible change in the oxidation state of a surface iron atom, due to the adsorption of molecules from the gas phase and their subsequent desorption, in which the Mössbauer spectrum of the adsorption complex is identified.*

Let us now consider the results obtained by adsorbing various molecules on the oxidized iron zeolite. All of the adsorption in-

teractions studied on the oxidized iron zeolite gave rise to a decrease in the QS of the main doublet. The decrease in QS is largest for H_2O followed by piperidine, ethanol, and ammonia. In addition a new peak was resolved in the spectrum of the oxidized material after piperidine adsorption. All of the adsorbates studied were condensable in the zeolite pores at room temperature at the equilibrium pressures investigated. Water and ammonia are small enough to enter all the cages of the zeolite and at the pressures used in the adsorption experiments would saturate the zeolite to form intracrystalline fluid. The apparent solvation of Fe^{2+} ions when water and ammonia were adsorbed on dehydrated Fe^{2+}–Y supports this conclusion. When the zeolite cavities are saturated with piperidine or ethanol, however, a solvation medium is not expected to form. The larger size of piperidine and ethanol which permits the adsorption of only about 5 and 9 molecules/supercage, respectively, compared to about 28 water and 23 ammonia molecules/supercage at saturation, can account for this difference. Although piperidine and ethanol cannot enter the sodalite cages or hexagonal prisms these adsorbates did cause small perturbations on the *outer* peaks due to Fe^{2+} ions in the hexagonal prisms when adsorbed in dehydrated Fe^{2+}–Y (*5*). These perturbations were attributed to long-range interactions resulting from adsorption on the zeolite framework. In the case of high spin Fe^{2+} the largest contribution to the electric field gradient is from the sixth *d*-electron when the ion is in a site of noncubic symmetry. Small changes in the charge distribution of the lattice due to adsorption interactions may only perturb slightly the electric field gradient seen by Fe^{2+}. As previously mentioned, however, high spin ferric ion is an $^6S_{5/2}$ state and sees only the electric field gradient produced by surrounding ions in the crystal. Thus the QS of this ion is more sensitive to changes in the charge distribution of the surrounding lattice ions.

The effect of water on the oxidized iron zeolite can be described as due to the addition of a large number of polar water molecules to the zeolite pores which alters the symmetry around the Fe^{3+} ion so as to reduce the electric field gradient at the iron nucleus. The QS of the Fe^{3+}-doublet depended strongly on the degree of hydration of the sample. Removing $\sim$½ of the zeolite water by room temperature evacuation increased the QS by 0.16 mm/sec whereas evacuation at 108°C which removes all but about 4% of the zeolite water increased the QS by 0.56 mm/sec compared to the wet sample. In the saturated state the zeolite pores are filled with water. Evacuation at room temperature removes most of the intracrystalline fluid medium but leaves about 16 water molecules/supercage adsorbed on the zeolite. This water is desorbed by evacuation at higher temperatures. Thus it appears that the largest effect on the charge distribution in the zeolite and hence on the QS arises from water which is adsorbed on the framework of the zeolite.

Since water can enter the sodalite cages of the zeolite we should also consider the possibility that hydrolysis of the oxidized species occurs according to the following equation.

$$Fe^{3+}—O^{2-}—Fe^{3+} + H_2O \rightleftarrows 2Fe^{3+}(OH)^- \quad (1)$$

The formation of the $Fe^{3+}(OH)^-$ groups combined with the effects of adsorbed water could account for the decrease in QS. Dehydration of the zeolite at high temperature would reverse Eq. (1) and regenerate the bridge. At some stage in the dehydration we would expect to have a mixture of the bridged species and the hydrolyzed species but there is no indication of two different species in the Mössbauer spectra up to 108°C evacuation. If Eq. (1) applies, either higher evacuation temperatures than 108°C are required for the dehydroxylation or the Mössbauer parameters of the two species are similar. We did not investigate evacuation temperatures in the intermediate range between 108 and 500°C. Evacuation at 500°C for 2 hr showed a continued increase in the QS of the oxidized doublet but some reduction to ferrous ion also occurred due to the desorption of oxygen.

The adsorption of ammonia, ethanol, and piperidine also caused decreases in the QS of the Fe^{3+} doublet but not as large as when

water was adsorbed. Although ammonia can enter the sodalite cages of the zeolite it had less effect on the QS than did piperidine and ethanol which are confined to the supercages. It is interesting to note that ammonia does not interact as strongly with Fe^{3+} ions as it does with Fe^{2+} ions (*5*) in Y zeolite. We would not expect ammonia to dissociate at room temperature and cause breakage of the Fe^{3+}–O^{2-}–Fe^{3+} bridge. We interpret the decrease in QS, when ammonia, piperidine, and ethanol are adsorbed, as due to interactions with the zeolite framework which alters the charge distribution of the lattice ions in such a way as to decrease the electric field gradient at the Fe^{3+} nucleus.

Although the computer analysis gave some indication of additional peaks in the spectra following ethanol and ammonia adsorption on oxidized iron zeolite, an unambiguous assignment could not be made. In the case of piperidine, however, an additional peak was clearly resolved. This is taken as evidence that the spectrum of the oxidized iron zeolite consists of more than one type of iron. Since we were unable to resolve the left half of the doublet giving rise to the peak at 2.3 mm/sec, the Mössbauer parameters for the doublet could not be determined. If the 2.3 mm/sec peak is the right half of a ferric doublet, the other peak would be located in the region −1.1 to −1.9 mm/sec to give an IS within the range expected for high spin Fe^{3+} ion. This would give rise to an unusually large QS for Fe^{3+} of >3.4 mm/sec. If the 2.3 mm/sec peak is the right half of a high spin ferrous doublet then the left half would fall in the region −0.4 to 0.5 mm/sec to give an IS within the range expected for high spin Fe^{2+}. Since computer fits and differential spectrum analysis did not indicate any peaks in the range −1.1 to −1.9 mm/sec and because such a large QS would be required for an assignment to Fe^{3+}, it seems more reasonable to assign the 2.3 mm/sec peak to the right half of a ferrous doublet. The adsorption of piperidine at room temperature is not expected to reduce ferric ions to ferrous ions but it is more probable that the ferrous species was already present in the oxidized sample. It is tempting to assign the 2.3 mm/sec peak to the right half of a quadrupole doublet from the interaction of piperidine with the $Fe^{2+}O^{2-}$ species which we indicated earlier may be present in the oxidized iron zeolite.

Next let us consider the oxidation of Fe^{2+}–Y at room temperature. This process requires the presence of both oxygen and water. Morice and Rees (*3*) also observed that oxidation of the ferrous ions produced on dehydration of Fe^{3+}–Y zeolite required both oxygen and water. In the case of Fe^{2+}–Y, it is not necessary that the ferrous ions be solvated for the oxidation to proceed since ferric ion was formed in a room temperature evacuated sample on exposure to oxygen. Room temperature evacuation of Fe^{2+}–Y forces most of the ions into localized positions. The oxidation at room temperature can proceed according to the following equation

$$2Fe^{2+} + \tfrac{1}{2}O_2 + H_2O \rightleftarrows 2Fe^{3+}(OH)^- . \qquad (2)$$

This is the reverse of Eq. (11) given by Morice and Rees.

When the sample oxidized in wet oxygen at room temperature was dehydrated at 410°C (Fig. 7c), three doublets were produced: the *inner* and *outer* peak ferrous doublets and a ferric doublet with parameters similar to that from Fe^{2+}–Y oxidized in dry oxygen at 400°C. Morice and Rees (*3*) also observed the formation of two ferrous species on dehydration of Fe^{3+}-exchanged Y zeolite (14% exchanged) at 360°C. Examination of their spectra for Fe^{3+}–Y dehydrated at 360°C shows striking similarity to those we obtained in Figs. 7c and 3c. A comparison of the Mössbauer parameters is shown in Table 2. There is good agreement between our results and those of Morice and Rees for the ferric doublets of the hydrated materials (Doublet A, Samples A and B) and for both of the ferrous species in the evacuated samples (Doublets 2 and 3, Samples C, D, and E). Their value for the QS of the ferric doublet (Doublet 1, Sample C) of the dehydrated material differs from that obtained in the present work (Doublet 1, Samples D and E). According to the results of Morice and

TABLE 2
COMPARISON OF MÖSSBAUER PARAMETERS FROM MORICE AND REES (3) AND FROM THIS WORK

	Morice and Rees (3) Sample A. Fe^{3+}–Y, as prepared by ion exchange		This work Sample B. Fe^{2+}–Y oxidized in dry oxygen at 400°C, hydrated at 25°C	
Doublet	IS[a]	QS	IS	QS
A	0.50	0.77	0.51	0.82

	Sample C. Fe^{3+}–Y, evacuated at 360°C		Sample D. Fe^{2+}–Y, oxidized in dry oxygen at 400°C, evacuated at 525°C		Sample E. Fe^{2+}–Y, oxidized in wet oxygen at 25°C, evacuated at 410°C	
			IS	QS	IS	QS
1	0.52	0.57	0.54	1.84	0.53	1.85
2	1.08	0.53	1.00	0.51	1.02	0.55
3	1.37	2.44	1.41	2.40	1.37	2.32

[a] IS and QS (mm/sec); IS with respect to ^{57}Co–Cr; data of Morice and Rees corrected to ^{57}Co–Cr by the addition of 0.15 mm/sec.

Rees the QS of the ferric doublet decreases on dehydration of the Fe^{3+}–Y samples (compare Doublet A of Sample A to Doublet 1 of Sample C). Our adsorption results on oxidized iron zeolite suggests, however, that removal of water leads to an increase in QS of the ferric doublet. It is not clear how Morice and Rees determined their parameters in Table 2. These authors represented their spectra as solid lines showing the envelope of the absorption curves. A comparison of our spectra for the Samples D and E, Table 2, with that of Sample C from Morice and Rees' work suggests that their spectra could be interpreted as containing a ferric doublet with QS similar to that which we observe.

To pursue this question, we prepared a sample of Fe^{3+}-exchanged Y zeolite following the procedure of Morice and Rees except that the final preparation was not dried at 100°C for 16 hr prior to the Mössbauer experiments. A sample of this material dehydrated at 360°C gave a nitrogen uptake at liquid nitrogen temperature of 7.45 mmole/g of dry zeolite indicating a small loss of crystallinity. The Mössbauer spectrum of the wet material gave a ferric doublet with IS, 0.53 mm/sec (^{57}Co–Cr), and QS, 0.74 mm/sec, in good agreement with that obtained by Morice and Rees (Doublet A, Table 2). When the Fe^{3+}–Y sample was heated to 350–360°C over an 8-hr period and then outgassed for 4 hr at this temperature to 10^{-5} Torr, spectrum 10a of Fig. 10 was obtained. This spectrum is very similar to that we obtained when a sample of Fe^{2+}–Y was oxidized in dry oxygen at 400°C, hydrated, and then evacuated 2 hr at 500°C (Fig. 5e). By comparing the weight of sample used and the area under the Mössbauer absorption curve in Fig. 10a with that of Fig. 5e, where the iron content of the sample was known, we estimate the exchange in the Fe^{3+}–Y sample to be ~75% if three sodium ions were replaced by one iron ion. The level of exchange of this sample is about 5 times that of the sample used by Morice and Rees. In spectrum 10a, the peaks at 0.8 and 2.5 mm/sec, which are close to the values expected for the left *inner* and the right *outer* peaks of dehydrated Fe^{2+}–Y and the asymmetry in the peaks at ~—0.3 and ~1.3 mm/sec indicate that some reduction to ferrous ions occurred. The degree of reduction to ferrous ions is not as great as that observed by Morice and Rees. More important, however, is the presence of a doublet with IS 0.5 mm/sec (^{57}Co–Cr), and QS, 1.9 mm/sec. The similarity of these parameters to those of Doublet 1, Samples D and E, Table 2

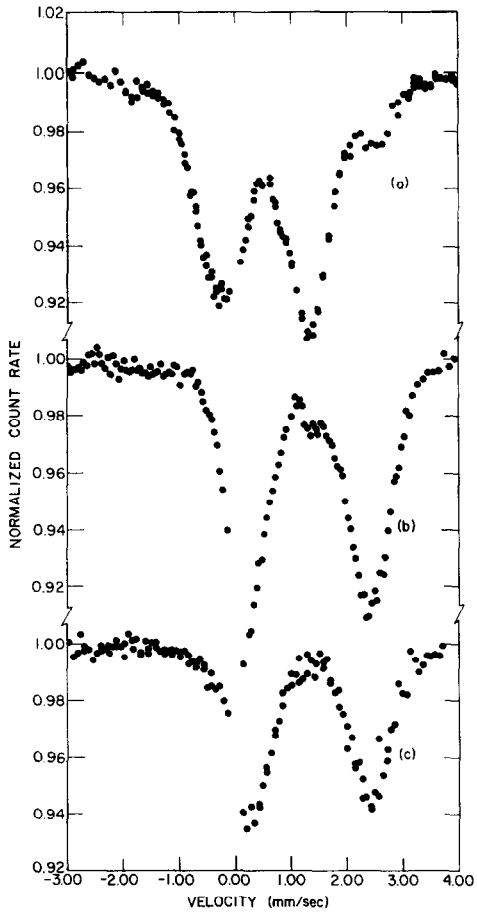

FIG. 10. Fe^{3+}-exchanged Y zeolite: (a) evacuated 350–360°C, 4 hr; (b) reduced in H_2, 400°C, 1 hr; (c) exposed to 15 Torr H_2O, room temperature. All spectra at room temperature and on the same sample.

strongly indicates that dehydrated Fe^{3+}–Y zeolite also contains ferric ions in the form of the iron–oxygen–iron bridges proposed earlier. In the 14% exchanged samples of Morice and Rees, lower concentrations of the Fe^{3+}–O^{2-}–Fe^{3+} bridges may have been present since a homogeneous exchange would have introduced only about one iron ion per sodalite cage. Thus some isolated ferric ions could have been present in their high temperature evacuated samples. If our interpretation of spectrum 10a is correct, then hydrogen reduction at 400°C of the sample giving that spectrum should give the characteristic spectrum of Fe^{2+}–Y zeolite. The result of the hydrogen reduction is shown in Fig. 10b. This spectrum resembles very closely that of the characteristic spectrum of Fe^{2+}–Y. The QS of the *outer* peaks and the intensity of the right *inner* peak are somewhat less than that of the characteristic spectrum of Fe^{2+}–Y, however. This may mean that the sample of Fig. 10b was not dehydrated to the same extent as that of samples giving the characteristic spectrum since the intensity of the *inner* peaks and the QS of the *outer* peaks was found earlier to increase with increasing degree of dehydration [see Fig. 2 in Ref. (*5*)]. This could also be due to the small loss of crystallinity which occurred during the exchange. The possibility that the peak at 1.4 mm/sec is due to the right half of a ferric doublet resulting from incomplete reduction should also be considered. To answer this question, the sample giving 10b was saturated with water at 15 Torr and room temperature. As shown in Fig. 10c, there is no indication of a ferric doublet with parameters expected for the hydrated material nor a large asymmetry in the lines that would occur if a ferric doublet were under the peak at 0.2 mm/sec and the ferrous lines were symmetric. In addition the spectral area of 10c is 40% less than that of 10b and the peak at 1.4 mm/sec was removed. These results also agree well with the behavior of Fe^{2+}–Y samples giving the characteristic spectrum (*4*, *5*).

The results of Morice and Rees and those of our own work strongly indicate that the same chemical states of iron are formed in Y zeolite by three very different paths. These are (i) oxidation of Fe^{2+}–Y at 400°C followed by evacuation at 525°C, (ii) oxidation of Fe^{2+}–Y at room temperature in wet oxygen followed by evacuation at 410°C, and (iii) dehydration of Fe^{3+}-exchanged Y zeolite at 360°C. The important observation of the present work which allows us to reconcile the findings of Morice and Rees with our own on Fe^{2+}–Y zeolite is that oxygen which is complexed with ferric ions in Y zeolite can be desorbed by high temperature evacuation with the formation of ferrous ions.

The changes observed on dehydration of our room temperature oxidized sample and those observed by Morice and Rees on de-

hydration of Fe^{3+}–Y appear to have a common explanation. According to Eq. (1), oxidation of the ferrous ions in Fe^{2+}–Y in the presence of water would form $Fe^{3+}(OH)^-$ groups. Since ferric ion has a strong tendency to hydrolyze (*20*), further hydrolysis of some of the $Fe^{3+}(OH)^-$ groups could occur as shown in the following equation.

$$Fe^{3+}(OH)^- + H_2O \rightleftarrows Fe^{3+}(OH)_2^{2-} + H^+. \quad (3)$$

The room temperature oxidized Fe^{2+}–Y would thus contain $Fe^{3+}(OH)^-$ and $Fe^{3+}(OH)_2^{2-}$ groups as well as some Fe^{2+} ions which were not oxidized by the room temperature treatment. The strong tendency for ferric ion to hydrolyze would also mean that the ferric-exchanged samples of Morice and Rees would contain mainly $Fe^{3+}(OH)^-$ and $Fe^{3+}(OH)_2^{2-}$ groups. Dehydration of the samples could then result in the formation of the *inner* and *outer* peak ferrous species and the bridged ferric ion species according to the following equations.

$$2Fe^{3+}(OH)^- \rightarrow Fe^{3+}—O^{2-}—Fe^{3+} + H_2O, \quad (4)$$

$$2Fe^{3+}(OH)^- \rightarrow 2Fe^{2+} + H_2O + \tfrac{1}{2}O_2, \quad (5)$$

$$2Fe^{3+}(OH)_2^{2-} \rightarrow Fe^{2+}—O^{2-}—Fe^{2+} + H_2O + \tfrac{1}{2}O_2, \quad (6)$$

$$Fe^{3+}(OH)^- + Fe^{3+}(OH)_2^{2-} \rightarrow Fe^{2+} + Fe^{2+}(OH)^- + H_2O + \tfrac{1}{2}O_2. \quad (7)$$

Equation (5) is essentially the same as that proposed by Morice and Rees to explain the formation of Fe^{2+} and it is supported by our observation that oxygen desorbs from the Fe^{3+} ions in Y zeolite on evacuation at high temperature.

Summary and Conclusions

Mössbauer spectroscopy and adsorption measurements show that dehydrated Fe^{2+}–Y zeolite adsorbs approximately one oxygen atom per two iron ions at 400°C with the formation of ferric ions. In keeping with our previously proposed model for Fe^{2+}–Y zeolite, the adsorption complex is described as a Fe^{3+}–O^{2-}–Fe^{3+} bridge located inside the sodalite cage. It appears that the Fe^{3+} ions occupy the *S I′* positions. All of the adsorbed oxygen can be removed by hydrogen reduction at 400°C with regeneration of the original dehydrated Fe^{2+}–Y zeolite; whereas, part of the oxygen is removed by evacuation of the oxidized sample at high temperature. The desorption of oxygen from the ferric ions by evacuation produces both of the ferrous species observed in dehydrated Fe^{2+}–Y.

Oxidation of the ferrous ions in Fe^{2+}–Y also occurs at room temperature but both water and oxygen are required. High temperature evacuation of a sample oxidized in this manner forms both of the ferrous species observed in dehydrated Fe^{2+}–Y as well as the oxidized species formed when Fe^{2+}–Y is oxidized in dry oxygen at 400°C.

The results of the present study allow us to reconcile and explain the oxidation–reduction behavior of both ferrous- and ferric-exchanged Y zeolites. The oxidation–reduction relationships between the ferric- and ferrous-exchanged Y zeolites are summarized in Fig. 11. The strong tendency for ferric ion to hydrolyze and the observation that oxygen complexed with ferric ions in Y zeolite can be desorbed accounts for the formation of ferrous ions in these materials by high temperature evacuation. As was

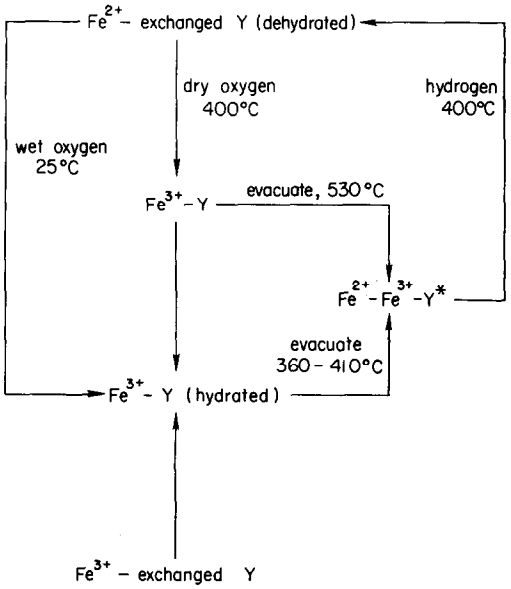

FIG. 11. Summary of oxidation–reduction relationships between ferrous- and ferric-exchanged Y zeolites. *The degree of conversion to ferrous ions was not the same for all samples.

previously suggested (*5*) nonframework O^{2-} and OH^- ligands are required to explain the behavior of Y zeolites containing ferric ions.

The implications of the present study for oxidation catalysis have yet to be assessed. The iron Y zeolite is an excellent oxygen carrier adsorbing ~3.5 times the amount of oxygen held by hemoglobin per gram of these materials. The reversible oxidation–reduction of iron ions exchanged into Y and other zeolites may allow the preparation of oxidation catalysts with interesting properties and selectivity.

Note added in proof: The infrared spectrum of our FeY sample in the presence of 200 Torr of CO showed the characteristic cation-specific CO band at 2198 cm^{-1} (C. L. Angell and P. C. Schaffer, *J. Phys. Chem.* **70,** 1413, (1966); on oxidation of the ferrous to the ferric form this band no longer appeared. (Private communication Drs. Angell and O'Hara).

Acknowledgments

This work has been supported by the Office of Army Research under contract DAHC 04 67 C 0045. One of us (WND) thanks the National Science Foundation for support in the form of a Graduate Fellowship while at Stanford University and the Air Force Office of Scientific Research for a Postdoctoral Research Award tenured at the University of California, Berkeley. Informative discussions with Professor D. A. Shirley of the University of California, Berkeley are gratefully acknowledged.

References

1. Gol'danskii, V. I., Suzdalev, I. P., Plachinda, A. S., and Shtyrkov, L. G., *Proc. Acad. Sci. USSR, Phys. Chem. Sect.* **169,** 511 (1968).
2. Gol'danskii, V. I., Neimark, I. E., Plachinda, A. S., and Suzdalev, I. P., *Int. Congr. Catal., 4th, Moscow, 1968; Symp. III Novosibirsk, prepr.,* No. 16.
3. Morice, J. A., and Rees, L. V. C., *Trans. Faraday Soc.* **64,** 1388 (1968).
4. Delgass, W. N., Garten, R. L., and Boudart, M., *J. Chem. Phys.* **50,** 4603 (1969).
5. Delgass, W. N., Garten, R. L., and Boudart, M., *J. Phys. Chem.,* in press.
6. Barrer, R. M., and Bratt, G. C., *J. Phys. Chem. Solids* **12,** 130 (1959).
7. Breck, D. W., *J. Chem. Educ.* **41,** 678 (1964).
8. Turkevich, J., *Catal. Rev.* **1,** 1 (1967).
9. Delgass, W. N., PhD dissertation, Stanford University, 1968.
10. Benson, J. E., and Boudart, M., *J. Catal.* **4,** 704 (1965).
11. Van Loef, J. J., *Physica (Utrecht)* **32,** 2102 (1966).
12. Brady, P. R., Duncan, J. F., and Mok, K. F., *Proc. Roy. Soc., Ser. A* **287,** 343 (1965).
13. May, L., *Advan. Chem. Ser.* **68,** 52 (1967).
14. Erickson, N. E., *Advan. Chem. Ser.* **68,** 86 (1967).
15. Huang, Y. Y., Benson, J. E., and Boudart, M., *Ind. Eng. Chem., Fundam.* **8,** 346 (1969).
16. Smith, J. V., Bennett, J. M., and Flanigen, E. M., *Nature (London)* **215,** 241 (1967).
17. Eulenberger, G. R., Shoemaker, D. P., and Keil, J. G., *J. Phys. Chem.* **71,** 1812 (1967).
18. Šimánek, E., and Šroubek, Z., *Phys. Rev.* **163,** 275 (1967).
19. Bennett, J. M., and Smith, J. V., *Mater. Res. Bull.* **23,** 865 (1968).
20. Cotton, F. Albert and Wilkinson, G., "Advanced Inorganic Chemistry." p. 715. Wiley (Interscience), New York, 1962.